

Hip Impingement of severe SCFE patients after in situ pinning causes decreased flexion and forced external rotation in flexion on 3D-CT

Till D Lerch^{1,2} , Young-Jo Kim², Ata Kiapour², Adam Boschung^{3,4}, Simon D Steppacher³, Moritz Tannast^{3,4}, Klaus A Siebenrock³, and Eduardo N Novais²

Abstract

Introduction: In situ pinning is an accepted treatment for stable slipped capital femoral epiphysis. However, residual deformity of severe slipped capital femoral epiphysis can cause femoroacetabular impingement and forced external rotation.

Purpose/questions: The aim of this study was to evaluate the (1) hip external rotation and internal rotation in flexion, (2) hip impingement location, and (3) impingement frequency in early flexion in severe slipped capital femoral epiphysis patients after in situ pinning using three-dimensional computed tomography.

Patients and methods: A retrospective Institutional Review Board-approved study evaluating 22 patients (26 hips) with severe slipped capital femoral epiphysis (slip angle > 60°) using postoperative three-dimensional computed tomography after in situ pinning was performed. Mean age at slipped capital femoral epiphysis diagnosis was 13 ± 2 years (58% male, four patients bilateral, 23% unstable, 85% chronic). Patients were compared to contralateral asymptomatic hips (15 hips) with unilateral slipped capital femoral epiphysis (control group). Pelvic three-dimensional computed tomography after in situ pinning was used to generate three-dimensional models. Specific software was used to determine range of motion and impingement location (equidistant method). And 22 hips (85%) underwent subsequent surgery.

Results: (1) Severe slipped capital femoral epiphysis patients had significantly ($p < 0.001$) decreased hip flexion ($43 \pm 40^\circ$) and internal rotation in 90° of flexion ($-16 \pm 21^\circ$, IRF- 90°) compared to control group ($122 \pm 9^\circ$ and $36 \pm 11^\circ$). (2) Femoral impingement in maximal flexion was located anterior to anterior–superior (27% on 3 o'clock and 27% on 1 o'clock) of severe slipped capital femoral epiphysis patients and located anterior to anterior–inferior (38% on 3 o'clock and 35% on 4 o'clock) in IRF- 90° . (3) However, 21 hips (81%) had flexion < 90° and 22 hips (85%) had < 10° of IRF- 90° due to hip impingement and 21 hips (81%) had forced external rotation in 90° of flexion (< 0° of IRF- 90°).

Conclusion: After in situ pinning, patient-specific three-dimensional models showed restricted flexion and IRF- 90° and forced external rotation in 90° of flexion due to early hip impingement and residual deformity in most of the severe slipped capital femoral epiphysis patients. This could help to plan subsequent hip preservation surgery, such as hip arthroscopy or femoral (derotation) osteotomy.

Keywords: Slipped capital femoral epiphysis, three-dimensional computed tomography, femoroacetabular impingement, in situ pinning

¹Department of Diagnostic, Interventional and Paediatric Radiology, University of Bern, Inselspital, Bern University Hospital, Bern, Switzerland

²Department of Orthopaedic surgery, Child and Young Adult Hip Preservation Program at Boston Children's Hospital, Harvard Medical School, Boston, MA, USA

³Department of Orthopaedic Surgery, Inselspital, University of Bern, Bern, Switzerland

⁴Department of Orthopaedic Surgery, HFR Fribourg—Cantonal Hospital, University of Fribourg, Fribourg, Switzerland

Date received: 22 November 2022; accepted: 13 July 2023

Corresponding Author:

Till D Lerch, Department of Diagnostic, Interventional and Paediatric Radiology, University of Bern, Inselspital, Bern University Hospital, Freiburgstrasse, Bern 3010, Switzerland.
 Emails: till.lerch@insel.ch; till.lerch@childrens.harvard.edu



Article summary

Article focus

Research questions addressed are as follows:

- Hip flexion and internal rotation (IR), and forced external rotation (ER);
- Impingement location;
- Impingement frequency in early flexion in severe SCFE patients after in situ pinning.

Key messages

- Restricted flexion and IR in 90° of flexion due to early hip impingement;
- Most of the severe SCFE patients had restricted flexion < 90° and had < 10° of IR in 90° of flexion and forced ER in 90° of flexion due to impingement;
- Proportion of anterior hip impingement in early flexion was high for severe SCFE patients after in situ pinning.

Strengths and limitations of this study

Strength: 3D-CT scan for 3D models, and standardized and validated method for range of motion and impingement simulation.

Limitation: Bone-to-bone contact for collision detection and small sample size.

Introduction

Slipped capital femoral epiphysis (SCFE) is a frequent hip disorder in adolescent patients with a high risk of disability.¹ In situ pinning is the conventional treatment for a stable SCFE.² In situ pinning provides stabilization of the growth plate followed by epiphysiodesis, and this treatment was associated with good Iowa hip outcome scores at long-term follow-up.^{3,4} However, this is different for hips with severe SCFE and the long-term hip outcome scores are lower, and radiographic progression to osteoarthritis is more prevalent than those with mild deformity.⁴⁻⁶ Although the deformity of the proximal femur may remodel after SCFE, the remodeling process occurs through impingement of the femur against the acetabular rim.⁷⁻⁹ SCFE-related femoroacetabular impingement (FAI) due to post-slip deformity can lead to acetabular cartilage defect, hip pain, limited motion, and ultimately to hip osteoarthritis.^{5,10-16}

The concept of SCFE-related FAI is not new.^{17,18} In 1999, Rab¹⁸ used a computerized 3D volume/surface model to describe the FAI secondary to SCFE as two different mechanisms: impaction and inclusion. On the one hand, impaction refers to metaphyseal impingement of the metaphysis against the acetabular labrum limiting the range of hip motion and leading to erosion of the acetabular labrum. On the other hand, inclusion happens once

the remodeled metaphyseal bump falls into the acetabulum and is associated with a high potential for erosion of the acetabular cartilage. Rab¹⁸ showed that relevant alterations in hip motion were necessary to compensate for the SCFE deformity.¹⁸ While little external rotation (ER) was needed to avoid metaphyseal impingement for a mild slip, more ER was needed with moderate and severe slips. A previous study of 23 patients simulated hip osteotomy and reported that the limitation of range of motion (ROM) was associated with the severity of the SCFE using computed tomography (CT).¹⁹ In addition, mild SCFE exhibited inclusion impingement, but for severe cases, the impaction impingement was the dominant mechanism due to the abutment of the prominent metaphysis on the acetabular rim. Another study using a 3D geometric model of acute SCFE deformity of one normal adolescent hip found that impingement occurred in all moderate and severe deformities, and it was noted anterosuperiorly on the acetabular rim.²⁰ Recently, patient-specific CT-based bony 3D models were used for dynamic simulation of hip ROM and were applied to patients with FAI,²¹ abnormal femoral torsion,²² and Legg–Calve–Perthes disease.²³

In this study, we sought to improve our understanding about the mechanism of FAI in severe SCFE patients treated with in situ pinning with a single cannulated screw. The specific aims of our study were (1) to determine post-operative hip ROM in external and internal rotation (IR) in flexion, (2) to identify the specific areas of femoral and acetabular impingement, and (3) to calculate the proportion of hips with impingement in early flexion using the patient-specific 3D-CT models after treatment with in situ pinning and comparing them to the contralateral uninjured hip as controls.

Patients and methods

Study design and population

This is a retrospective Institutional Review Board (IRB)-approved study. We searched our tertiary pediatric hospital database to identify patients treated for SCFE between 2000 and 2018. Patients between 8 and 15 years of age who had a postoperative CT scan (Figure 1) of the pelvis that included the femoral condyles after in situ pinning were included. The indications for acquiring a CT during the study period included an assessment of the residual symptomatic deformity, planning for the surgical treatment, and deciding whether to conduct a subcapital realignment or other procedures, such as osteoplasty or intertrochanteric osteotomy. The epiphysis-diaphysis angle, according to Southwick,²⁴ was measured on the preoperative lateral radiographs to classify SCFE as mild (<30°), moderate (30°–60°), or severe (>60°). We excluded patients with mild (slip angle < 30°) and moderate SCFE (slip angle 30°–60°), patients with only preoperative CT available (no previous treatment performed), and inadequate CT

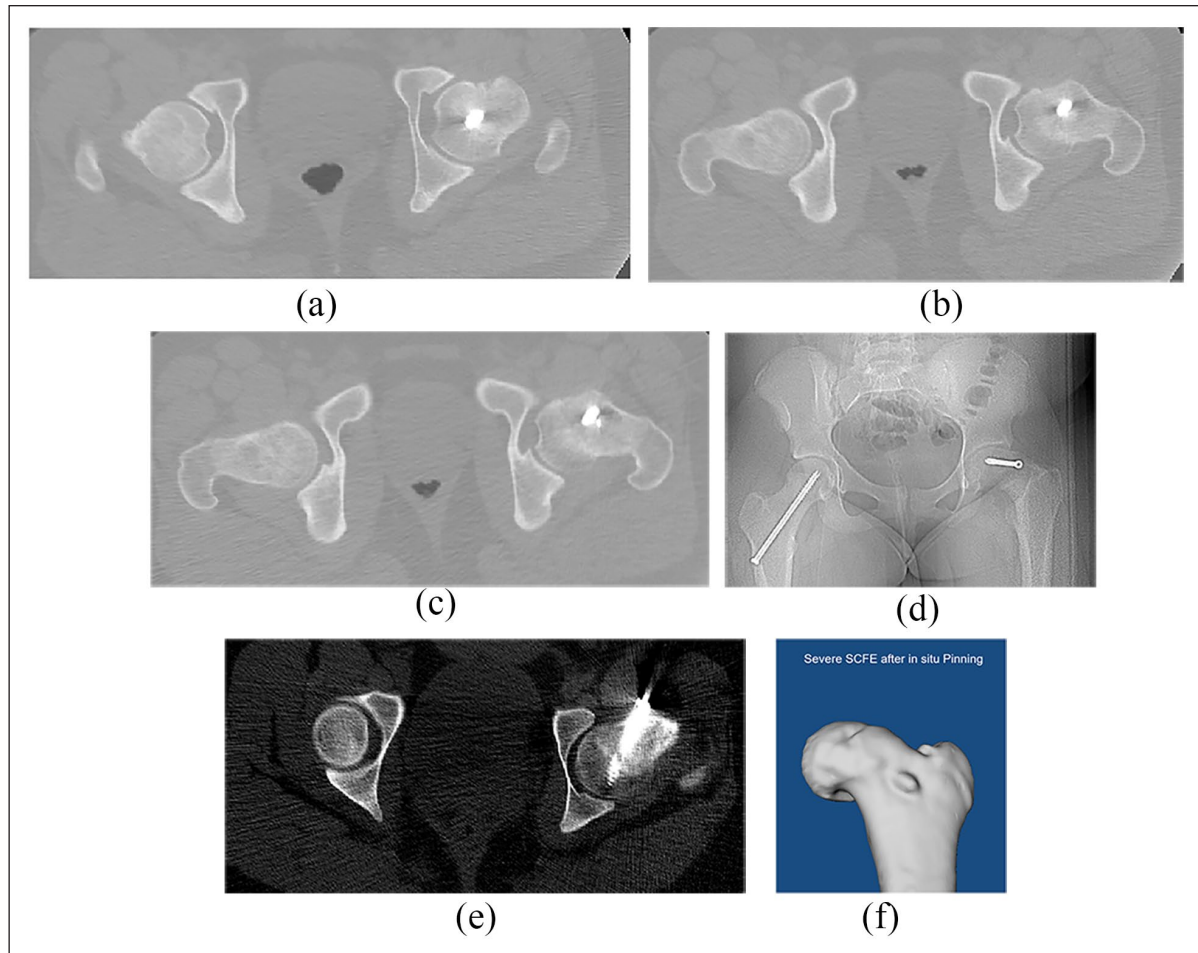


Figure 1. (a–f) Pelvic CT scan of a patient with severe SCFE treated with in situ pinning (a–c). Anteroposterior (AP) pelvis radiograph (d) and corresponding pelvic CT scan (e) of a second patient with severe SCFE treated with in situ pinning. Femoral CT-based 3D model of another patient with severe SCFE after previous in situ pinning (f).

images (e.g. CT of unilateral hip joint or missing femoral condyles). Of 123 patients with SCFE and CT imaging available, 101 patients were excluded, yielding the final cohort of 22 patients with severe SCFE treated with in situ pinning with postoperative pelvic CT image that included the femoral condyles. There were 15 male patients (58%), with a mean age of 13 ± 2 years at the time of SCFE diagnosis and 14 ± 3 years at the CT scan (Table 1). Four patients (15%) had bilateral SCFE, yielding 26 hips included in the analysis. Out of the 26 hips with severe SCFE, 22 (85%) were chronic, and 20 (67%) were stable. Surgery was performed for 22 hips (85%) after the CT scan. The contralateral hips of 15 patients with unilateral SCFE of a previous study²⁵ were used as a control group.

Imaging and 3D impingement simulation

All patients underwent standardized anteroposterior (AP) and frog-leg or cross-table lateral radiographs and CT of the pelvis (Figure 1), including the distal femoral

condyles. Mean femoral anteversion was -7° , minimal femoral anteversion was -36° (femoral retroversion), and maximum was 61° . Femoral anteversion was measured according to the Murphy method. Overall, 11 (42%) hips had absolute femoral retroversion $< 0^\circ$. An osseous 3D model of the proximal femur and the pelvis (Figure 1(f)) of every patient was generated using the software Amira (Visage Imaging Inc, Carlsbad, CA, USA). Threshold-based bone segmentation was performed by two independent observers (TDL and AB). The two observers were independent and were not the treating physicians of the patients. The acetabular reference coordinate system was the modified anterior pelvic plane (APP), a virtual plane formed by the pubic tubercles and the inferior iliac spines (Supplemental Table 1) and a tilt angle of 20° as previously described.²¹ The femoral reference coordinate system was defined by the knee center, both femoral condyles and the center of the femoral head.²⁶

Specific collision detection software was used for 3D impingement simulation to determine the degree of

Table 1. Demographic information of the patient series.

Parameter	Value
Total hips (patients)	41 (37)
Total hips with severe SCFE (patients)	26 (22)
Total hips of asymptomatic controls (patients)	15 (15)
Age at imaging (years)	14 ± 3 (10–21)
Age at SCFE diagnosis (years)	13 ± 2 (10–17)
Gender (% male of all hips)	58
Side (% left of all hips)	73
Height (cm)	167 ± 10 (152–184)
Weight (kg)	82 ± 15 (62–126)
Body mass index (kg/m ²)	29 ± 5 (21–45)

SCFE: slipped capital femoral epiphysis.

Continuous values are displayed as mean ± standard deviation and range in parenthesis.

impingement-free hip flexion (Figure 2(a)) and IR with the hip in 90° of flexion (Figure 2(b)) in severe SCFE hips after in situ pinning and control hips. The amount of necessary ER in 90° of flexion (Figure 2(c)) was calculated for severe SCFE patients. The details and algorithms of the used software were described in previous studies and are based on the equidistant method and are listed in Supplemental Table 1. The impingement location was analyzed for every patient individually. The impingement location was assessed in a standardized manner with a clockface system that was also used intraoperatively: inferior was defined 6 o'clock and represents the acetabular notch on the acetabular side; 3 o'clock represents anterior (for both right and left hips), as per Tannast et al.'s study.²³ To calculate the proportion of hips with impingement in pure flexion without rotation, impingement was recorded in 10° increments between 60° and 90° of flexion. The proportion of hips with impingement at each given hip flexion was recorded and compared to control group. All patients were evaluated with the equidistant method using personalized CT-based 3D bone models and validated collision detection software.²⁷ Based on a cadaveric investigation, the impingement collision can be detected with a mean accuracy of 2.6° ± 2.5°. The intra- and interobserver measurements for this software for IR in 90° of flexion and for flexion were excellent (> 0.9)²¹ in a validation study.

Statistical analysis

Statistical analysis was performed using Winstat software (R. Fitch Software, Bad Krozingen, Germany). The data were assessed for normal distribution with the Kolmogorov–Smirnov test. Because not all the parameters were normally distributed, we used nonparametric tests for comparison. To compare demographic and radiographic data, ROM, or location of impingement, we used the Mann–Whitney U

test. The chi-square test was used to compare the frequency of impingement at different degrees of hip flexion.

Results

Mean flexion was significantly ($p < 0.001$) decreased in hips with severe SCFE after in situ pinning ($43^\circ \pm 40^\circ$, range -20° to 120°) compared with uninvolved contralateral hips ($122^\circ \pm 9^\circ$, range 107° to 138° , Figure 2(a)). Similarly, mean IR with the hip in 90° of flexion was significantly ($p < 0.001$) decreased in severe SCFE patients treated with in situ pinning ($-16^\circ \pm 21^\circ$, range -55° to 35°) compared to the control group ($36^\circ \pm 11^\circ$, range 21° – 55° , Figure 2(b)). The -16° of IR with the hip in 90° flexion represent the forced ER in 90° of flexion (Figure 2(c)).

In maximum hip flexion, the impingement zones on the femur were located more anterosuperior (between the 1 and 3 o'clock) in the hips with severe SCFE after in situ pinning compared ($p < 0.001$) to the uninvolved contralateral group (5 o'clock). (Figure 3(a)) Impingement in maximum hip flexion was similarly concentrated on the acetabular 2 o'clock zone for hips with severe SCFE after in situ pinning (69%) and the control hips (93%) (Figure 3(b)).

In maximum IR with the hip in 90° of flexion, the femoral location of impingement differed significantly ($p < 0.001$) between hips with severe SCFE after in situ pinning and uninvolved contralateral hips. (Figure 4(a)) The impingement location on the acetabulum was more superior (between 12 and 2 o'clock) in hips with severe SCFE after in situ pinning compared ($p < 0.001$) to the control group (2 o'clock) (Figure 4(b)).

Regarding the third aim of this study, no uninvolved contralateral hip showed impingement with flexion from 60° to 90°. The proportion of hips with detected impingement with pure flexion (no rotation) increased with increasing degrees of hip flexion of severe SCFE patients after in situ pinning. A significantly higher proportion ($p < 0.001$) of severe SCFE hips after in situ pinning showed impingement in flexion from 60° to 90° (Table 2) compared to the control group.

Discussion

The residual deformity of the proximal femur after in situ pinning for severe SCFE may partially remodel through impaction or inclusion impingement between the metaphyseal bump and the acetabular rim.^{8,18} However, impingement after severe SCFE is known to cause articular cartilage damage and is associated with long-term osteoarthritis.^{3–5,11,28} In this study, we used postoperative CT images to create 3D models of patients with severe SCFE after in situ pinning to better understand the pathomechanics of FAI by measuring the impingement-free hip motion

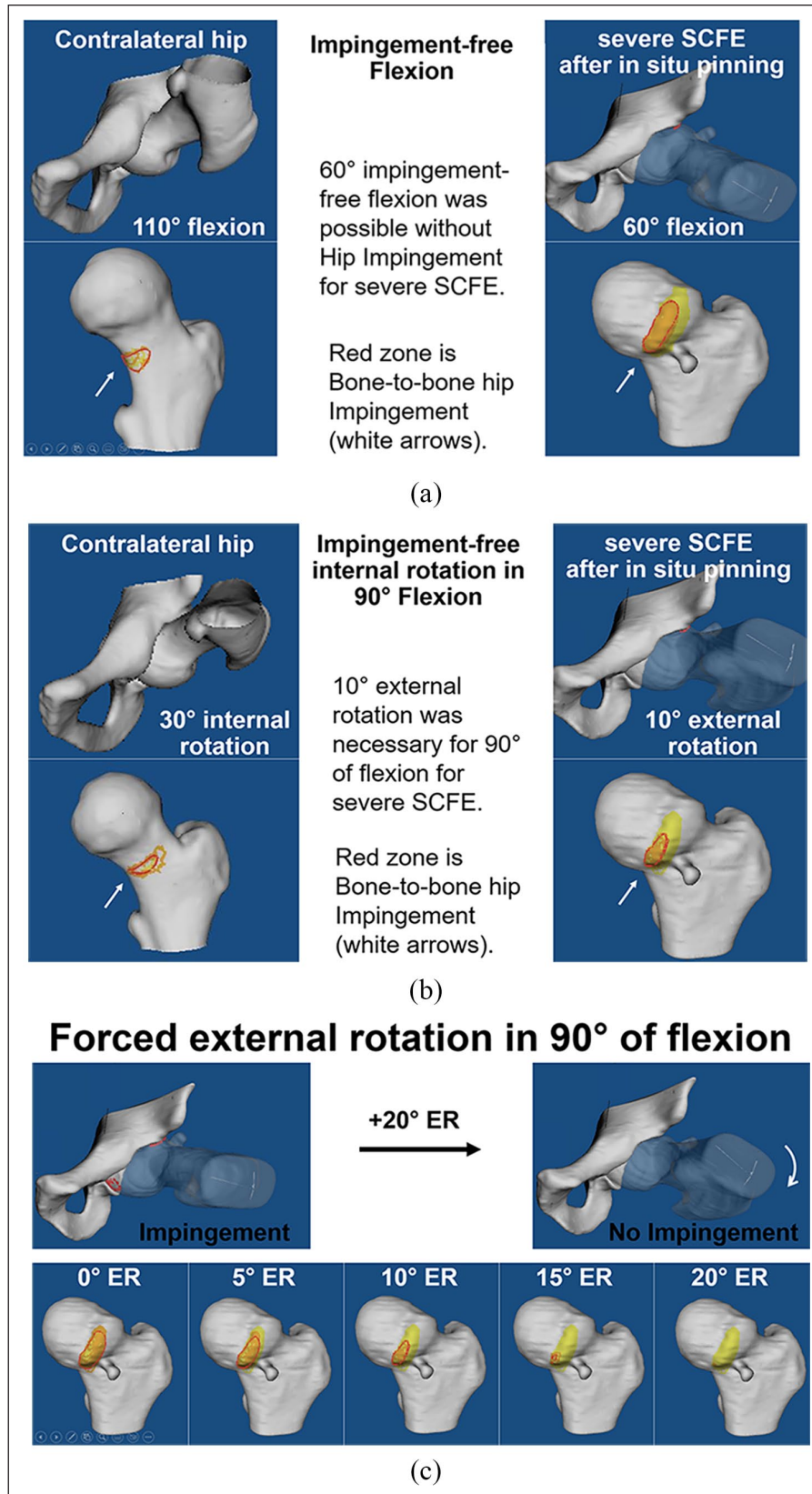


Figure 2. (a) CT-based 3D models of a patient with severe SCFE after previous in situ pinning is shown in impingement-free flexion. (b) Impingement-free simulation of 90° flexion was performed and (c) impingement-free 90° of flexion was achieved with 16° of external rotation.

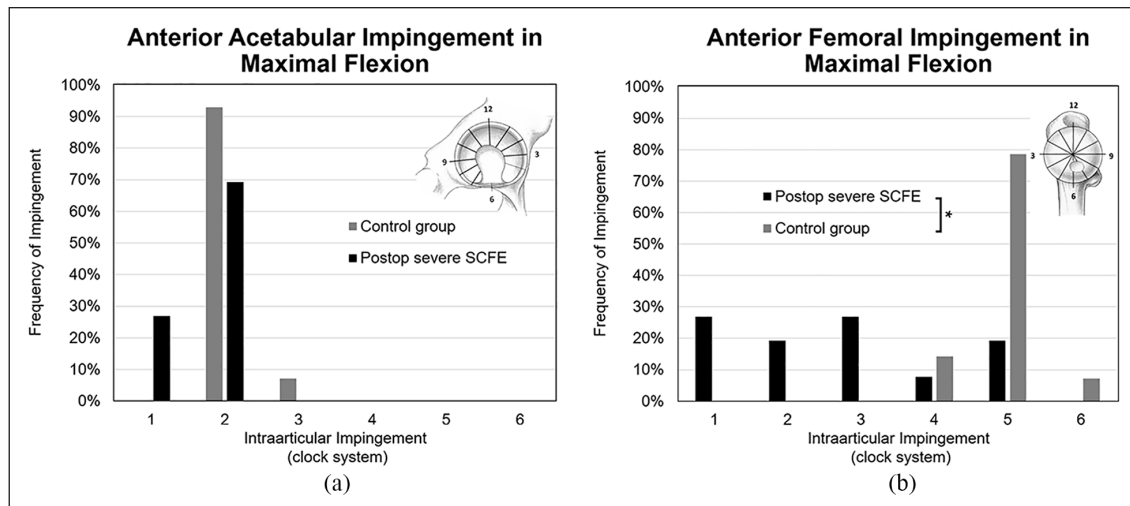


Figure 3. (a) Acetabular and (b) femoral impingement location is shown in maximal flexion using a patient-specific osseous CT-based 3D model of a patient with severe SCFE after previous in situ pinning.

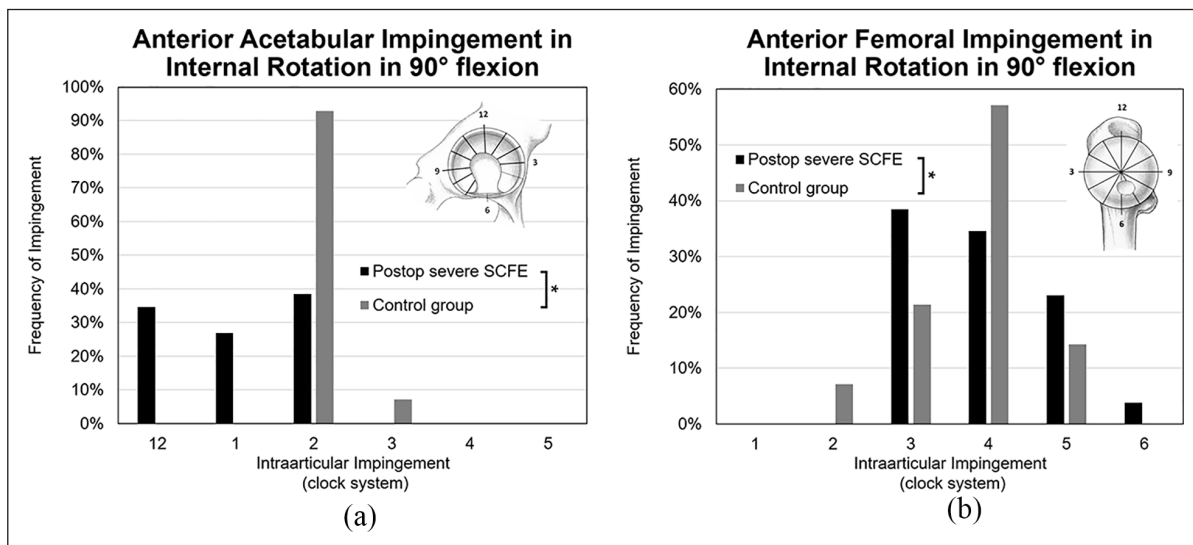


Figure 4. Acetabular (a) and femoral (b) impingement location is shown in maximal internal rotation with the hip in 90° of flexion using a patient-specific osseous CT-based 3D model of a patient with severe SCFE after previous in situ pinning.

Table 2. Frequency of impingement in early flexion is shown (without rotation) using patient-specific osseous CT-based 3D models of patients with severe SCFE after previous in situ pinning.

Parameter	SCFE patients	Asymptomatic control	p
Total hips	26	15	
Impingement in 60° of flexion	69%	0%	0.001
Impingement in 70° of flexion	73%	0%	0.001
Impingement in 80° of flexion	77%	0%	0.001
Impingement in 90° of flexion	81%	0%	0.001

SCFE: slipped capital femoral epiphysis.

and assessing the specific location of impingement on the femur and acetabulum compared to the uninvolved contralateral hip.

We found that IR with the hip in 90° of flexion and mean hip flexion were significantly decreased in hips with severe SCFE following in situ pinning compared to the

normal hips. Mamisch et al.²⁹ simulated hip motion in 31 patients with SCFE who had CT imaging before surgical treatment and found that although for mild SCFE, the hip motion was comparable to the unaffected side, for severe SCFE, there was near complete loss of normal motion. They found lower motion in flexion ($4.4^\circ \pm 12.4^\circ$) but higher measurements of IR ($8.4^\circ \pm 26.2^\circ$) compared to the current study reporting mean of $43^\circ \pm 40^\circ$ flexion and mean IR with the hip in 90° of flexion of $-16^\circ \pm 21^\circ$. Another study¹⁹ performed simulations with different proximal femoral osteotomies and investigated ROM after SCFE using a specific software and CT image of 19 patients with moderate and severe SCFE. Again here, that study showed lower mean flexion ($4^\circ \pm 13^\circ$) but higher IR ($8^\circ \pm 23^\circ$) compared to the results of the current study. The slight discrepancy between ours and previous studies findings may be related to the software used in those studies but also to the fact that hips with severe SCFE do not have a homogeneous deformity. Rather, the location of the epiphysis in relation to the metaphysis varies in hips with severe SCFE and is influenced by the remodeling process. Jones et al.³⁰ classified hips based on the anterior head and neck profile and showed that hips that failed to remodel the anterior head-neck had decreased range of IR compared to hips that remodel. Mamisch et al.²⁹ noted that the Jones type 3 deformity (the femoral epiphysis is positioned dorsal in relation to the metaphysis) is associated with impaction type of impingement and severely decreased hip flexion and IR compared to type 2 Jones deformity (epiphysis and metaphysis are on the same level in ventral direction).

In this study, the location of impingement zones on the femur with hip flexion was more anterosuperior in the hips with severe SCFE after in situ pinning compared to the uninvolved contralateral group. With IR in 90° hip flexion, the impingement zones on the acetabulum were located more superiorly (between 12 and 2 o'clock, Figure 4) in hips with severe SCFE. There is limited literature analyzing the location of the impingement in hips with SCFE. Recent studies have used patient-specific 3D models to analyze the slip direction³¹ and for 3D printing³² to simulate corrective surgery. Femoral and acetabular osseous impingement locations have been reported for hips with cam and pincer FAI.²³ However, specifically to severe SCFE, few studies investigated individual hip impingement location in IR and flexion. A study reporting intraoperative evaluation of articular cartilage damage in patients undergoing surgical treatment for symptomatic FAI post-SCFE has described the location of damage in the anterior–superior acetabulum. This is consistent with the results of acetabular impingement location (Figures 3 and 4) found in the current study, and it provides a biomechanical explanation for the previously reported acetabular cartilage damage.

The proportion of hips with severe SCFE after in situ pinning with detected impingement with pure flexion (no

rotation) increased with increasing degrees of hip flexion. It is well accepted that patients with severe SCFE walk with an outward rotation of the lower extremity and to flex the hip, it is mandatory that the hip rotates externally – the so-called Drehmann³³ sign. The found results in the current study of -16° of IR in 90° of flexion represents 16° of forced ER. Our findings are in line with Kamegaya et al.'s³⁴ study that investigated 80 SCFE patients (92 hips) treated with in situ pinning and noted that 25% of hips with Jones type A deformity, 75% of hips with Jones type B, and 100% with hips with Jones type C exhibited the Drehmann sign. The authors assessed three patients with a dynamic 3D-CT during testing for Drehmann sign and noted a direct contact between the femoral metaphysis and the acetabulum as early as in 30° of flexion. With additional flexion (at 70° of flexion), the location of impingement changed as the femur rotated externally. We believe that the limited impingement-free range of hip flexion in hips with severe SCFE may be an essential component to the disfunction often observed in these patients. Notably, Kamegaya et al. reported after a mean 12-year-follow up that 7 (25%) of the 28 patients with a positive Drehmann sign reported pain or limp, while patients with a negative Drehmann sign reported no pain.

Our results showed that hips with severe SCFE exhibit severe limitation of hip motion and a high proportion of anterior impingement with simple hip flexion after in situ pinning. However, this treatment purely does not alter the problem acutely. In severe SCFE, complete resolution of impingement would require either an intertrochanteric osteotomy,^{35–37} a subcapital realignment through a modified Dunn³⁸ or a combined approach using the surgical hip dislocation with a femoral osteotomy.³⁹ However, these procedures may be associated with surgical complications, and because of the stabilization and the good short-term outcomes of SCFE patients after in situ fixation,^{3,4} most pediatric orthopedic surgeons prefer to treat severe SCFE with percutaneous pinning. We believe that, in the setting of limited hip motion and with an obligatory ER test (Drehmann sign), patients with severe SCFE should be counseled for repetitive follow-up examinations to monitor for the development of symptoms and radiographic signs of osteoarthritis. Independent of the planned surgical treatment for symptomatic FAI in patients with previously pinned severe SCFE, the severe limitations of hip motion due to early hip impingement and the location of impingement described in our study should be considered for preoperative planning.

This study has limitations. First, the software for collision detection calculates the osseous ROM, without considering soft tissue (labrum, muscles, or cartilage). This is unavoidable using pelvic CT scans for 3D modeling and could be integrated using MR in the future. It is possible that the clinical ROM for SCFE patients could be decreased. In addition, pelvic CT scans have a considerable radiation exposure, especially for young patients. Low-dose CT scans or MR could be used to reduce

radiation exposure in the future. Unfortunately, clinical ROM could not be assessed for all patients in the current study due to hip pain and the retrospective nature of the chart review. In addition, the used asymptomatic control group of a previous study does not necessarily have a “normal” hip joint because of the theoretical risk of a contralateral slip. Patients analyzed in this study were from a pediatric university center in Boston, USA with limited generalizability and potential selection bias for referred patients. No detailed patient-related hip outcome scores or clinical examinations were evaluated because this was not the aim of this study. Hip pain was reported by all patients at the time of CT acquisition and 85% of them underwent subsequent hip preservation surgery. Finally, we did not evaluate the effect of other anatomic parameters, including pelvic tilt, and acetabular and pelvic morphology, which could also affect hip ROM.

Conclusion

Patient-specific 3D bone models of severe SCFE patients showed restricted flexion and IR of the hip at 90° of flexion and a high proportion of forced ER in 90° of flexion and a high frequency of impingement with isolated hip flexion after in situ pinning. This study also describes the specific location of impingement in hips with severe SCFE after in situ pinning. Patient-specific 3D models of hips with severe SCFE may facilitate standardized diagnosis and surgical planning for a hip preservation surgery that can stabilize the slip and treat the impingement, avoiding additional damage to the acetabular cartilage and hopefully preventing the development of osteoarthritis. However, future investigations will be needed to investigate whether patient-specific designed corrections are safe and impact treatment outcomes in patients with severe SCFE deformity.

Declaration of conflicting interests

The author(s) declared no potential conflicts of interest with respect to the research, authorship, and/or publication of this article.

Ethical approval

Each author certifies that his or her institution approved the human protocol for this investigation, that all investigations were conducted in conformity with ethical principles of research, and that informed consent for participation in the study was obtained.

Funding

The author(s) disclosed receipt of the following financial support for the research, authorship, and/or publication of this article: T.D.L. has received funding from the Swiss National Science Foundation (Early Postdoc.Mobility P2BEP3_195241).

ORCID iD

Till D Lerch  <https://orcid.org/0000-0002-0475-0269>

Supplemental material

Supplemental material for this article is available online.

References

1. Lehmann CL, Arons RR, Loder RT, et al. The epidemiology of slipped capital femoral epiphysis: an update. *J Pediatr Orthop* 2006; 26(3): 286–290.
2. Millis MB and Novais EN. In situ fixation for slipped capital femoral epiphysis: perspectives in 2011. *J Bone Joint Surg Am* 2011; 93(Suppl. 2): 46–51.
3. Boyer DW and Mickelson MR, Ponseti IV. Slipped capital femoral epiphysis. Long-term follow-up study of one hundred and twenty-one patients. *J Bone Joint Surg Am* 1981; 63(1): 85–95.
4. Carney BT, Weinstein SL and Noble J. Long-term follow-up of slipped capital femoral epiphysis. *J Bone Joint Surg Am* 1991; 73(5): 667–674.
5. Castañeda P, Ponce C, Villareal G, et al. The natural history of osteoarthritis after a slipped capital femoral epiphysis/the pistol grip deformity. *J Pediatr Orthop* 2013; 33(Suppl. 1): S76–S82.
6. Larson AN, Sierra RJ, Yu EM, et al. Outcomes of slipped capital femoral epiphysis treated with in situ pinning. *J Pediatr Orthop* 2012; 32(2): 125–130.
7. Dawes B, Jaremko JL and Balakumar J. Radiographic assessment of bone remodelling in slipped upper femoral epiphyses using Klein's line and the alpha angle of femoral-acetabular impingement: a retrospective review. *J Pediatr Orthop* 2011; 31(2): 153–158.
8. O'Brien ET and Fahey JJ. Remodeling of the femoral neck after in situ pinning for slipped capital femoral epiphysis. *J Bone Joint Surg Am* 1977; 59(1): 62–68.
9. Ganz R, Parvizi J, Beck M, et al. Femoroacetabular impingement: a cause for osteoarthritis of the hip. *Clin Orthop Relat Res* 2003; 417: 112–120.
10. Helgesson L, Johansson PK, Aurell Y, et al. Early osteoarthritis after slipped capital femoral epiphysis. *Acta Orthop* 2018; 89(2): 222–228.
11. Sink EL, Zaltz I, Heare T, et al. Acetabular cartilage and labral damage observed during surgical hip dislocation for stable slipped capital femoral epiphysis. *J Pediatr Orthop* 2010; 30(1): 26–30.
12. Leunig M, Casillas MM, Hamlet M, et al. Slipped capital femoral epiphysis: early mechanical damage to the acetabular cartilage by a prominent femoral metaphysis. *Acta Orthop Scand* 2000; 71(4): 370–375.
13. Leunig M, Fraitzl CR and Ganz R. Early damage to the acetabular cartilage in slipped capital femoral epiphysis. Therapeutic consequences. *Orthopade* 2002; 31(9): 894–899.
14. Abraham E, Gonzalez MH, Pratap S, et al. Clinical implications of anatomical wear characteristics in slipped capital femoral epiphysis and primary osteoarthritis. *J Pediatr Orthop* 2007; 27(7): 788–795.
15. Stulberg S, Cordell L, Harris W, et al. Unrecognized childhood hip disease: a major cause of idiopathic osteoarthritis of the hip. In: *The Hip: proceedings of the third open scientific meeting of the Hip Society*, St. Louis, MO, 1975.
16. Örtengren J, Peterson P, Svensson J, et al. Persisting CAM deformity is associated with early cartilage degeneration after

- Slipped Capital Femoral Epiphysis: 11-year follow-up including dGEMRIC. *Osteoarthr Cartil* 2018; 26(4): 557–563.
17. Richolt JA, Teschner M, Everett PC, et al. Impingement simulation of the hip in SCFE using 3D models. *Comput Aid Surg* 1999; 4(3): 144–151.
 18. Rab GT. The geometry of slipped capital femoral epiphysis: implications for movement, impingement, and corrective osteotomy. *J Pediatr Orthop* 1999; 19(4): 419–424.
 19. Mamisch TC, Kim YJ, Richolt J, et al. Range of motion after computed tomography-based simulation of intertrochanteric corrective osteotomy in cases of slipped capital femoral epiphysis: comparison of uniplanar flexion osteotomy and multiplanar flexion, valgisation, and rotational osteotomies. *J Pediatr Orthop* 2009; 29(4): 336–340.
 20. Jones CE, Cooper AP, Doucette J, et al. Relationships between severity of deformity and impingement in slipped capital femoral epiphysis. *J Pediatr Orthop* 2017; 37(4): 272–278.
 21. Tannast M, Kubiak-Langer M, Langlotz F, et al. Noninvasive three-dimensional assessment of femoroacetabular impingement. *J Orthop Res* 2007; 25(1): 122–131.
 22. Siebenrock KA, Steppacher SD, Haefeli PC, et al. Valgus hip with high antetorsion causes pain through posterior extraarticular FAI. *Clin Orthop Relat Res* 2013; 471(12): 3774–3780.
 23. Tannast M, Hanke M, Ecker TM, et al. LCPD: reduced range of motion resulting from extra- and intraarticular impingement. *Clin Orthop Relat Res* 2012; 470(9): 2431–2440.
 24. Southwick WO. Slipped capital femoral epiphysis. *J Bone Joint Surg Am* 1984; 66(8): 1151–1152.
 25. Lerch TD, Kim YJ, Kiapour AM, et al. Limited hip flexion and internal rotation resulting from early hip impingement conflict on anterior metaphysis of patients with untreated severe SCFE using 3D Modelling. *J Pediatr Orthop* 2022; 42(10): e963–e970.
 26. Murphy SB, Simon SR, Kijewski PK, et al. Femoral anteversion. *J Bone Joint Surg Am* 1987; 69(8): 1169–1176.
 27. Puls M, Ecker TM, Tannast M, et al. The Equidistant Method—a novel hip joint simulation algorithm for detection of femoroacetabular impingement. *Comput Aid Surg* 2010; 15(4–6): 75–82.
 28. Ziebarth K, Leunig M, Slongo T, et al. Slipped capital femoral epiphysis: relevant pathophysiological findings with open surgery. *Clin Orthop Relat Res* 2013; 471(7): 2156–2162.
 29. Mamisch TC, Kim YJ, Richolt JA, et al. Femoral morphology due to impingement influences the range of motion in slipped capital femoral epiphysis. *Clin Orthop Relat Res* 2009; 467(3): 692–698.
 30. Jones JR, Paterson DC, Hillier TM, et al. Remodelling after pinning for slipped capital femoral epiphysis. *J Bone Joint Surg Br* 1990; 72(4): 568–573.
 31. Bland DC, Valdovino AG, Jeffords ME, et al. Evaluation of the three-dimensional translational and angular deformity in slipped capital femoral epiphysis. *J Orthop Res* 2020; 38(5): 1081–1088.
 32. Cherkasskiy L, Caffrey JP, Szewczyk AF, et al. Patient-specific 3D models aid planning for triplane proximal femoral osteotomy in slipped capital femoral epiphysis. *J Child Orthop* 2017; 11(2): 147–153.
 33. Drehmann F. Das Drehmannsche zeichen eine klinische untersuchungsmethode bei epiphyseolysis capitis femoris zeichenbeschreibungen, ätiopathogenetische gedanken, klinische erfahrungen. *Z Orthop* 1979; 1979: 118333–118344.
 34. Kamegaya M, Saisu T, Nakamura J, et al. Drehmann sign and femoro-acetabular impingement in SCFE. *J Pediatr Orthop* 2011; 31(8): 853–857.
 35. Schai PA, Exner GU and Hänsch O. Prevention of secondary coxarthrosis in slipped capital femoral epiphysis: a long-term follow-up study after corrective intertrochanteric osteotomy. *J Pediatr Orthop B* 1996; 5(3): 135–143.
 36. Oduwole KO, de Sa D, Kay J, et al. Surgical treatment of femoroacetabular impingement following slipped capital femoral epiphysis: a systematic review. *Bone Joint Res* 2017; 6(8): 472–480.
 37. Southwick WO. Osteotomy through the lesser trochanter for slipped capital femoral epiphysis. *J Bone Joint Surg Am* 1967; 49(5): 807–835.
 38. Novais EN, Maranhão DA, Heare T, et al. The modified Dunn procedure provides superior short-term outcomes in the treatment of the unstable slipped capital femoral epiphysis as compared to the inadvertent closed reduction and percutaneous pinning: a comparative clinical study. *Int Orthop* 2019; 43: 669–675.
 39. Spencer S, Millis MB and Kim YJ. Early results of treatment of hip impingement syndrome in slipped capital femoral epiphysis and pistol grip deformity of the femoral head-neck junction using the surgical dislocation technique. *J Pediatr Orthop* 2006; 26(3): 281–285.